*N. Knee**

Coping with Residual Stresses in the Integrity Assessment of an As-Welded Repair

REFERENCE Knee, N., **Coping with residual stresses in the integrity assessment of an as-welded repair**, *Defect Assessment in Components – Fundamentals and Applications*, ESIS/EGF9 (Edited by J. G. Blauel and K.-H. Schwalbe) 1991, Mechanical Engineering Publications, London, pp. 909–923.

ABSTRACT One of a series of large scale tests on pressure vessels is described, in which a defect was deliberately introduced into an as-welded (i.e., not stress relieved) repair weld. The behaviour of the vessel during pressurisation to failure was carefully monitored, and the actual performance compared with theoretical predictions. The influence of residual welding stresses on ductile crack growth from defects is discussed in the light of the results of this test, and of previous tests in the series. The tests have confirmed that residual stresses can exert a significant effect on the growth of fatigue cracks. However, in tests for which the failure mechanism is predominantly controlled by collapse of the remaining ligament, the development of plasticity during pressurisation to failure will tend to remove any local residual stresses.

Introduction

The assessment of structures containing defects is routinely carried out on power station components within the UK using the methods described in the defect assessment procedure 'R6' (1). One of the most difficult aspects is to incorporate the effects of residual stresses in a safe manner, without making unduly conservative assumptions about the levels of stress that may be present.

A series of large scale bursting tests have been carried out on pressure vessels containing semi-elliptic defects. The purpose of these tests has primarily been to validate the R6 defect assessment method (1), and previous tests in the series have also been the subject of comparative analyses performed by members of the European Group on Fracture (2)–(4). In each test the vessel and defect geometry have been similar, but the material properties and residual stresses in the region of the defect have been varied. In the fourth test in the series, which is described in this paper, the influence of residual welding stresses arising from a repair weld was studied. The weld procedure used is intended to be suitable for the repair of PWR primary pressure circuit components without the need for post weld heat treatment.

The objectives of the present test were to provide further validation of R6 as a defect assessment procedure, and to investigate the effect of residual stresses on defect growth and load carrying capacity. As part of the post-test analysis,

* Technology Division, Nuclear Electric, Canal Road, Gravesend, Kent, DA12 2RS, UK.

the sensitivity of the results to uncertainties in various input parameters was studied, and the experimental results compared with theoretical predictions. The experiment was also intended as a practical trial of the novel as-welded repair technique.

Experimental procedure

Vessel preparation

The test vessel (Fig. 1) was fabricated from A533B steel, and consisted of a cylindrical test section 1.6 m long with a wall thickness of 84.5 mm, welded to hemispherical end caps. A longitudinal repair weld was made in the cylindrical section, in a 90 degrees included angle repair preparation machined to half the wall thickness on the inner surface (bore). A length of repair to the same procedure was made in a test plate at the same time. An automated tungsten inert gas (TIG) process was used, following a six-layer procedure (5) developed by Babcock and Wilcox (USA) and the Central Electricity Generating Board. The procedure is designed to produce grain refinement and tempering of the heat affected zone (HAZ). The test section was welded to the hemispherical ends after completing the repair and grinding the weld cap smooth. No post weld heat treatment was carried out.

The defect was introduced into the outer surface on the centre-line of the repair weld by machining a starter notch and extending a crack by fatigue. This was achieved by pressure cycling with the vessel filled with water at ambient temperature. Fatigue crack growth was monitored continuously using the changes in compliance measured by a clip gauge across the mouth of the notch. Ultrasonic inspection was also carried out at intervals. The compliance measurements during fatigue crack growth showed a change in slope suggesting that significant crack closure attributable to residual stresses was occurring at pressures below 15 MPa.

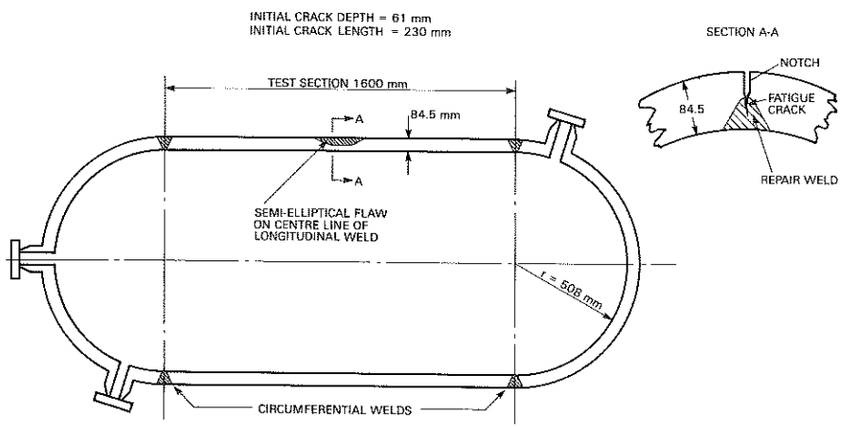

Fig 1 Geometry of test vessel

Fatigue cycling was continued until the crack length at the deepest point was 63 mm, measured by an ultrasonic time of flight technique. The crack shape was predicted to be rather irregular from an ultrasonic survey, with negligible crack extension appearing to have occurred at the quarter points. Full details of the pre-crack shape were revealed after pressurisation to failure.

Material properties

Charpy tests on specimens of parent plate, HAZ and repair weld metal were carried out (Fig. 2) which showed that the transition behaviour of the weld metal and of parent plate was similar, and that the HAZ exhibited superior

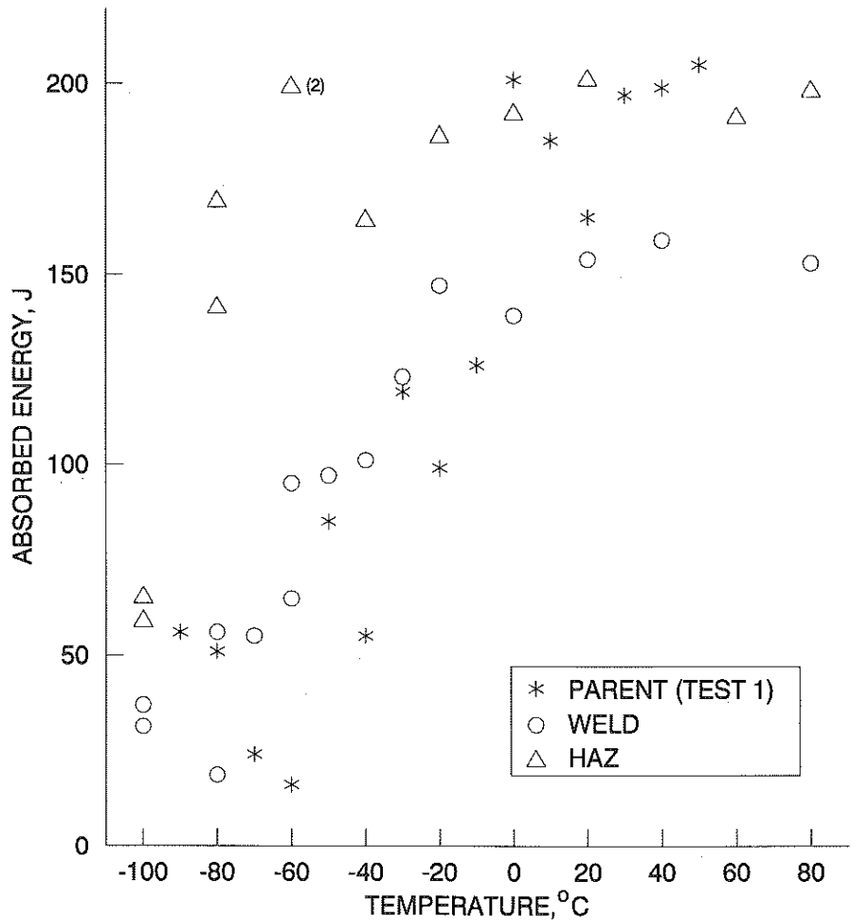

Fig 2 Charpy impact test results

transition behaviour. All results were 100 percent ductile at temperatures above 20°C and to be sure of ductile behaviour in the vessel test a test temperature of 50°C was chosen. The J resistance curve for the repair weld metal was measured using a single specimen unloading compliance technique, and the results are shown in Fig. 3. A side-grooved compact tension was used, with a thickness of 25 mm. The specimen orientation was such that growth at the deepest point of the semi-elliptic flaw was modelled. Expressions of the form $J = b\ (\Delta a)^c$ were fitted to the experimental data for weld metal, and for parent plate (2), where Δa is the crack extension in mm, J is the value of the J integral in kN/m, and b and c are constants. The results of the curve fits are given in Table 1, together with strength data measured on standard tensile specimens.

Residual stresses

Residual stresses were measured on the surfaces of the cylindrical section of the test vessel shell prior to welding on the hemispherical ends, and on the test plate. The centre-hole drilling technique was used, and the locations of the 13 measurement points are shown in Fig. 4. No measurements were made on the bore near the defect location as these may have influenced the growth of the defect during the test, and the stresses on the bore at the defect location were inferred from measurements made near the end of the shell. The measured surface residual stresses are given in Table 2, and represented by vector dia-

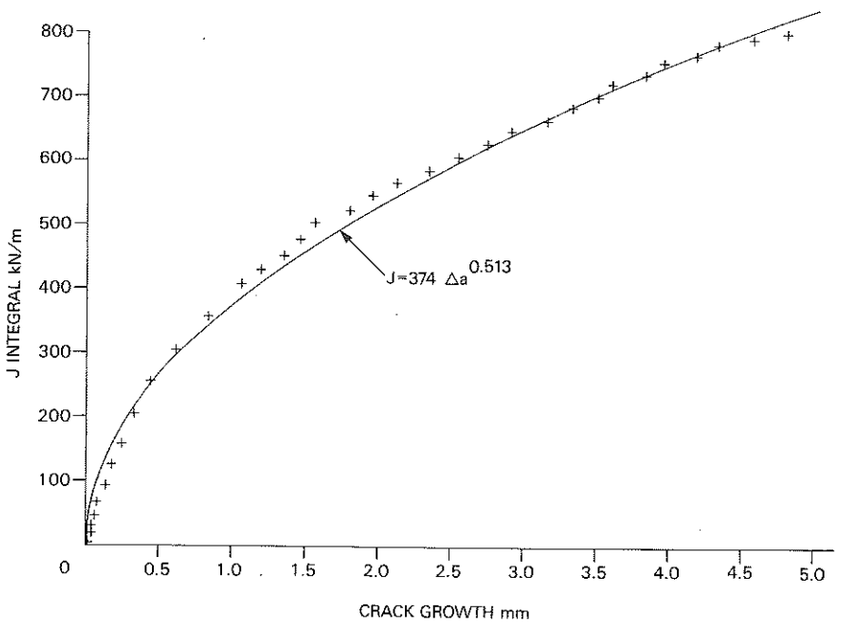

Fig 3 Unloading compliance results (J resistance curve)

Table 1 Material properties for parent plate and repair weld. Parameters b and c define the crack growth resistance curve $J = b\ (\Delta a)^c$, where Δa is in mm and J is in kN/m

	Parent plate	*Repair weld*
0.2 percent proof stress (MPa)	556	616
Tensile strength (MPa)	691	709
Coefficient b (kN/m)	890	374
Exponent c	0.572	0.513
Initiation toughness $J_{0.2}$ (kN/m)	284	193

grams in Fig. 5. All of the measured surface stresses were tensile, and the stresses in the test plate followed a similar pattern to those in the vessel shell, although the magnitude of the stresses was up to 200 MPa greater in the test plate. There was no evidence of a systematic variation in residual stress between the defect location and near the end of the shell.

The general pattern is of hoop tensile stresses on both inner and outer surfaces, with measured values in the range 320 to 553 MPa, combined with axial tensile stresses which are small on the inner surface (53–120 MPa) and large on the outer surface (503–712 MPa). The mean residual hoop stresses on the inner and outer surfaces in the region of the defect were estimated as follows. The results from locations 8, 9, and 10 were averaged to give a mean hoop stress on the outer surface of 472 MPa. No equivalent measurements were

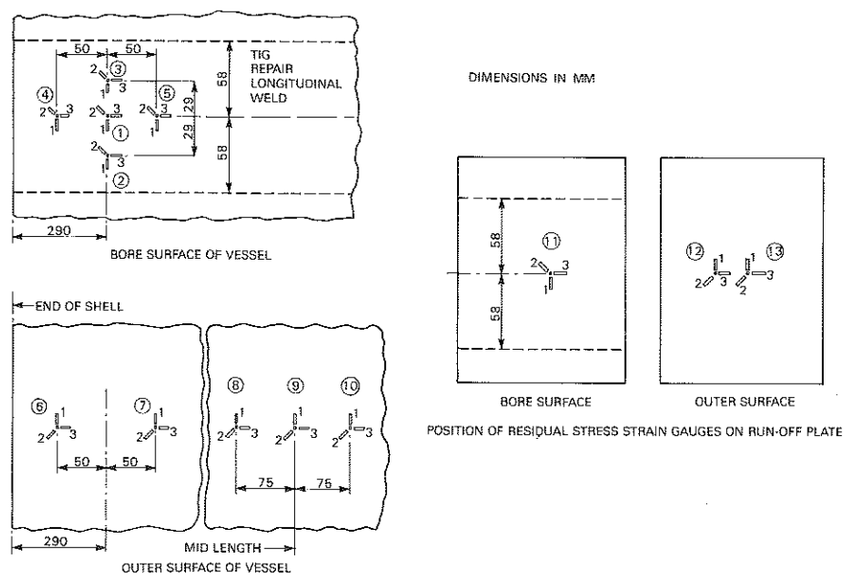

Fig 4 Locations of strain gauge rosettes for residual stress determination

Table 2 Residual stresses measured on the surfaces of the vessel shell and test plate

Location reference	Principal stresses σ_{max} (MPa)	Principal stresses σ_{min} (MPa)	Orientation relative to σ_{max} (degrees)	Directional stresses hoop (MPa)	Directional stresses axial (MPa)
1	635	425	75.3	438	621
2	669	553	89.4	553	669
3	712	502	−89.0	502	712
4	599	424	79.3	430	593
5	526	414	63.1	437	503
6	335	51	−4.8	333	53
7	404	48	6.9	399	53
8	328	108	−11.0	320	116
9	409	118	4.4	408	120
10	489	104	4.9	486	106
11	735	391	84.5	394	732
12	648	276	4.5	646	279
13	575	133	12.2	555	153

made on the inner surface, but the outer surface measurements were comparable at the defect location and near the end of the shell. Therefore the average of all the measurements on the inner surface near the end of the shell was taken as representative of the mean hoop stress on the inner surface at the defect location, i.e., a stress of 405 MPa.

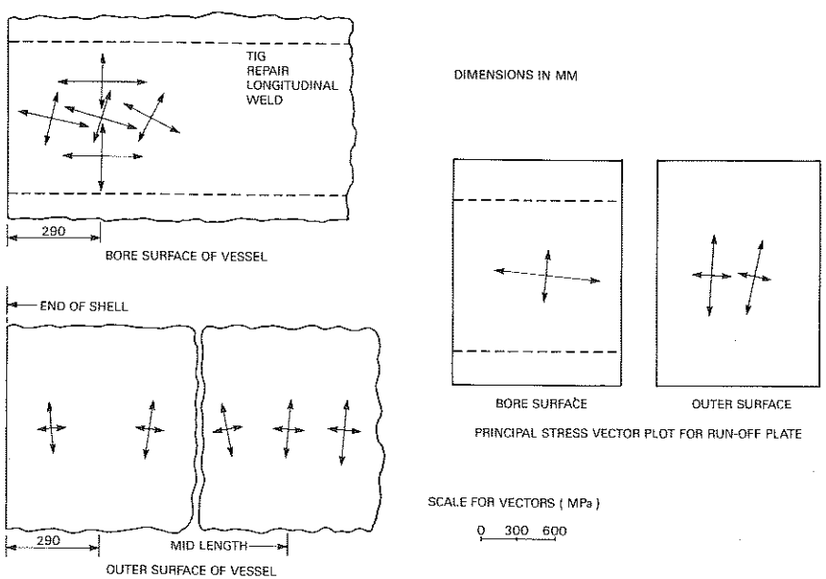

Fig 5 Vector diagram of surface residual stresses on pressure vessel and test plate

Pressurisation to failure

During the pressurisation to failure of the vessel, the following data were monitored and logged at intervals.

- Internal pressure.
- Crack mouth opening displacement (CMOD) at the middle and at one quarter of the defect length.
- Outer surface strain, using eight rosettes distributed around the vessel.
- Crack depth at the mid-length of the defect, using the ultrasonic time of flight technique.
- Temperature at various locations on the vessel.

The vessel and contents were heated to 50°C, and temperatures allowed to equilibrate for several hours before starting the test. A record of internal pressure as a function of CMOD is given in Fig. 6. A number of depressurisations (labelled A–F), both planned and unplanned, occurred during the test, which served to mark the progress of the crack. Studies of the interaction of tearing and fatigue have shown that these additional fatigue cycles are unlikely to affect the extent of ductile crack extension **(6)**. The maximum internal pressure sustained by the vessel was 83.4 MPa.

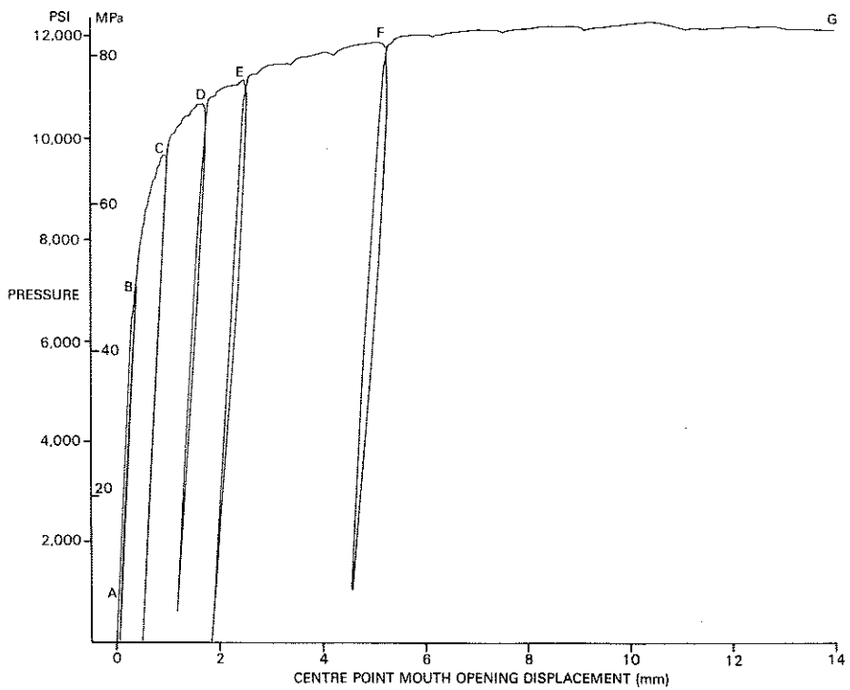

Fig 6 Plot of pressure against crack mouth opening displacement

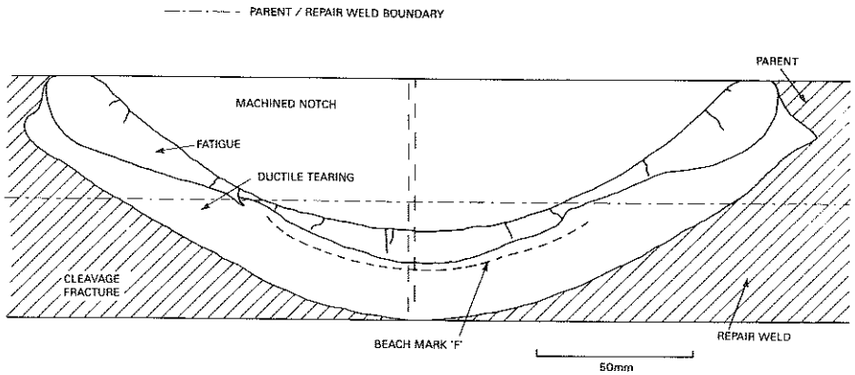

Fig 7 Map of fracture appearance

The test was stopped at point G which corresponds to the defect penetrating the wall and leakage occurring. The crack depth at the deepest point was monitored by an ultrasonic time of flight method, with send and receive probes mounted across the mouth of the notch. The results were corrected to account for the increases in CMOD and hence probe separation during the test. The time of flight method gave an initial crack depth of 63 mm, and an initial wall thickness of 84.5 mm. At the end of the test the crack tip and back face indications were coincident at 77 mm, confirming that considerable plastic necking of the ligament had occurred. The crack depth at the maximum internal pressure of 83.4 MPa was predicted to be about 73 mm, using the ultrasonic method.

After the test, the defect and surrounding area were cut from the vessel and the fracture surface revealed by breaking open the ligament at a low temperature. The fracture appearance is shown in Figs 7 and 8. The shapes of the starter notch, the fatigue crack and of ductile growth during the test are clearly defined. Multiple initiation of fatigue cracks occurred, giving rise to a number of steps on the fatigue fracture surface perpendicular to the crack growth direction. Fatigue crack growth was retarded near the interface between the parent metal and repair weld. The crack depth at the deepest point measured on the fracture surface was 61 mm. This value was used in the post-test analysis.

Beach marks in the ductile tearing region, parallel to the fatigue crack front, were apparent within the repair weld metal. The line of the beach mark generated during the depressurisation marked F on Fig. 6 is shown on Fig. 7. Closer examination revealed three further beach marks, corresponding to depressurisations C, D, and E (Fig. 9). No visible beach marks were generated during depressurisations A and B, which occurred prior to the initiation of ductile tearing. The beach marks provide a valuable indicator of the progress of the crack during the test. They were used to construct a load/crack exten-

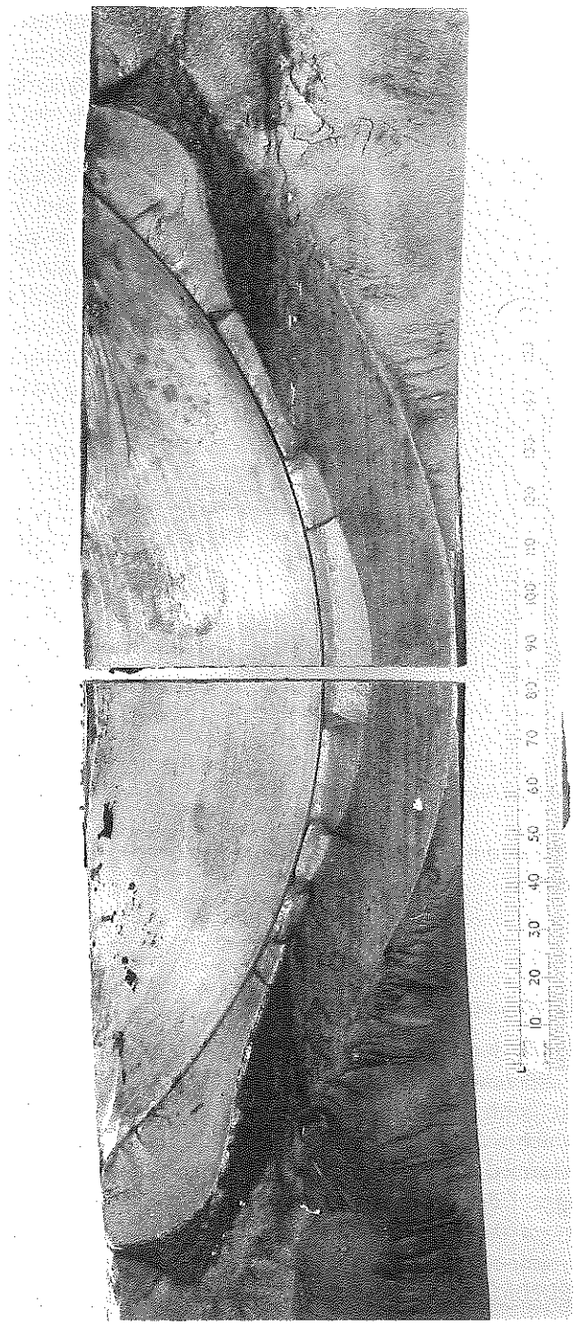

Fig 8 Fracture appearance

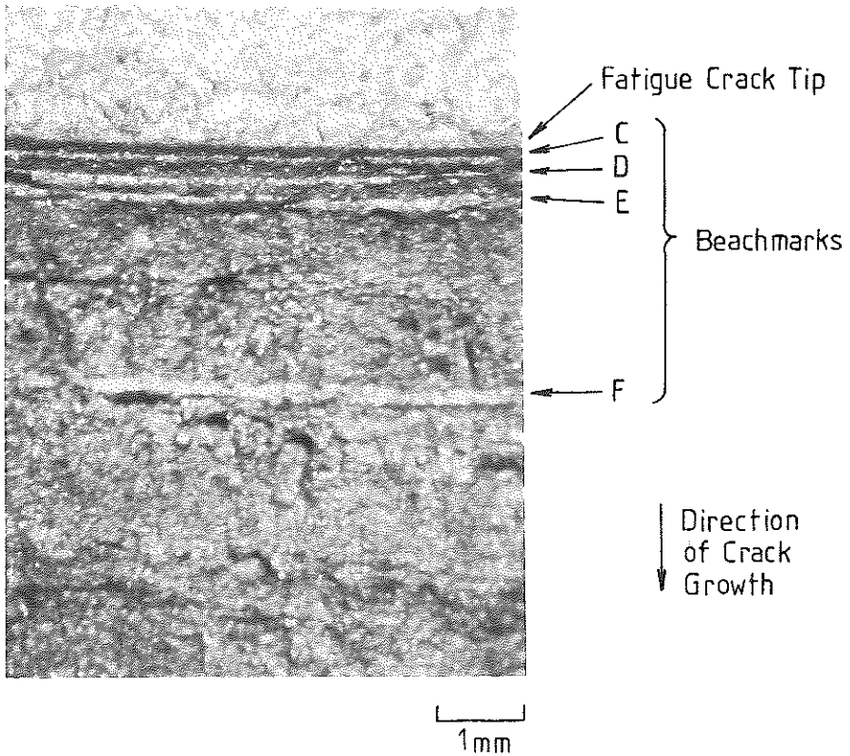

Fig 9 Optical micrograph showing beach marks near deepest point of defect

sion curve for the structure which is compared with theoretical predictions in the following section.

Analysis

Prediction of performance

All of the analysis which follows makes use of the R6 methodology **(1)**, with the important difference that best estimate input data are used to predict behaviour. This contrasts with the intended application of R6 for failure avoidance in which a conservative assessment of the limiting conditions for a structure is performed using lower bound materials data. The general failure assessment diagram described as Option 1 in R6 was used throughout. The initial geometry of the structure is shown in Fig. 1. The fatigue crack was modelled as a semi-ellipse, and it was assumed that the aspect ratio of the ellipse remained constant as the defect extended. The only primary stress in the structure arises from the pressure load, which generates hoop and axial

stresses in the cylindrical shell, whose magnitude for the uncracked body can be simply calculated from elastic theory. A best estimate of the secondary (residual) stresses was made by taking the mean measured surface values, and using data obtained in the Welding Institute **(7)** on a repair weld made to a similar procedure to give the form of the through thickness variation in stress (Fig. 10). Crack tip stress intensity factors at the deepest point were calculated by a weight function method from solutions derived by Raju and Newman **(8)**, using curve fits to the stress data as a function of depth for both primary and secondary stress. The collapse solution was that derived by Kiefner *et al.* **(9)**.

The resulting predictions of vessel performance using R6 are compared with the experimental results in Fig. 11 and Table 3. Failure occurs at high values of the collapse parameter, L_r, with initiation at $L_r = 0.81$, and instability at $L_r = 1.03$. The analysis has underestimated the maximum load sustained, and the pressure at crack initiation, taken as a crack extension of 0.2 mm. The experimental initiation value is based on linear interpolation from beach marks C and D.

Sensitivity study

The sensitivity of the results to uncertainties in the material properties and levels of residual stress was undertaken. This showed that, as expected for a structure failing close to collapse, the results were sensitive to the tensile properties, but less sensitive to the parameters in the crack growth resistance curve. The results were also sensitive to the initial crack size.

A variety of alternative assumptions for the form of the through thickness residual hoop stress distribution were tested. The best estimate distribution

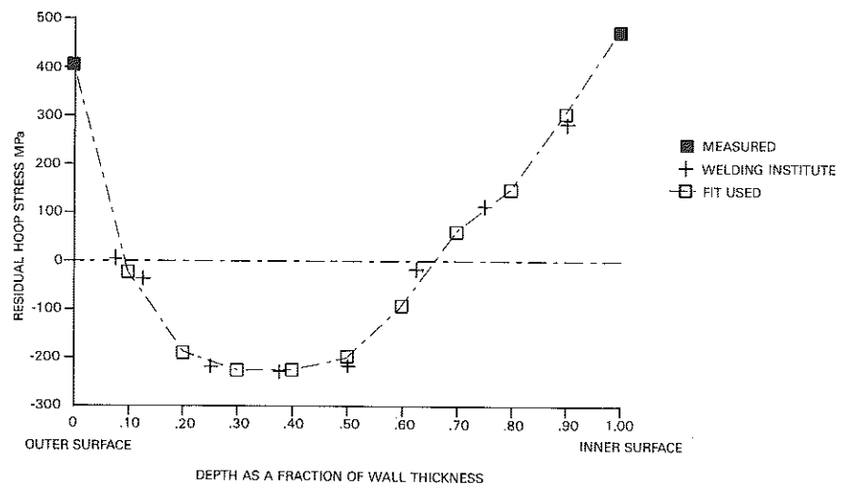

Fig 10 Through thickness residual stress distribution (based on Welding Institute results and measured surface values)

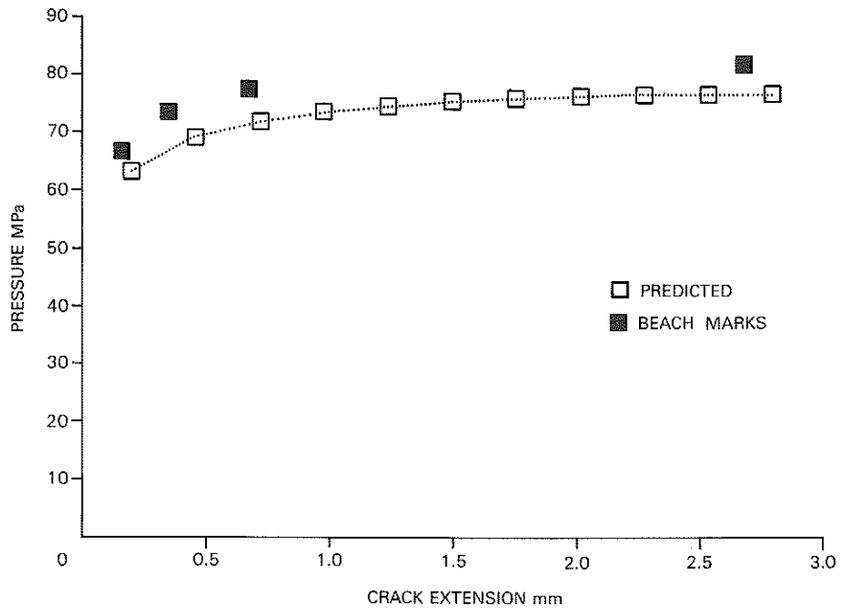

Fig 11 Comparison of predicted and measured crack extension

which is tensile at both surfaces and compressive in the middle of the section is predicted to give rise to crack closure at the deepest point of the defect. Therefore a reduction in initiation and maximum pressure is predicted if the residual stress is ignored. Assuming tensile residual stresses across the section produces further reduction in failure pressures, with a more marked effect on initiation than on maximum pressure. The extent of ductile tearing at instability increases from 2.6 mm for the best estimate residual stress distribution to

Table 3 Comparison of predicted and experimental performance of the pressure vessel

Load case	*Initiation pressure (MPa)*	*Maximum pressure (MPa)*	*Crack extension at max. pressure (mm)*
1	63.0	76.0	2.6
2	59.3	74.7	4.7
3	40.1	67.8	4.6
4	22.8	61.2	4.6
Experiment	68.0	83.4	>2.7

Key to load cases:
(1) Best estimate residual stress distribution.
(2) No residual stress.
(3) Residual stress increases linearly from 0 at the inner surface to 250 MPa at the outer surface.
(4) Uniform residual stress of 250 MPa across the wall thickness.

almost 5 mm for the other load cases assumed. Accurate information about the actual crack growth at maximum load was not obtained during the experiment, and Fig. 6 shows that CMOD was increasing rapidly close to maximum load. However, beach mark F proves that at least 2.7 mm of crack extension had occurred at 81.0 MPa, well before maximum pressure. The ultrasonic time of flight measurements indicated that about 10 mm of crack growth had occurred at maximum load.

Prediction of flaw shape development

The initial fatigue crack shape was affected by the residual stresses present, with enhanced growth in the parent metal near the outer surface, and retarded growth near the interface between parent metal and repair weld. This behaviour correlates at least qualitatively with the assumed best estimate residual stress distribution (Fig. 10), in which there are tensile stresses at the surface and compressive stresses near the mid-wall. Introduction of the defect and fatigue crack growth will have caused some redistribution of the residual stresses, but this has been neglected.

The final flaw shape when the vessel wall was breached appears to be little influenced by the presence of residual stresses or the change in material properties between the parent metal, HAZ, and weld metal. It appears that as in the previous test **(4)**, the development of extensive plasticity in the remaining ligament eliminates the local elastic residual stresses produced during welding. The final profile has a similar 'canoe' profile to that produced in previous tests **(2)–(4)**, and in other pressure vessel tests **(10)**. Lack of through thickness constraint prevents any crack growth at the surface, but enhanced subsurface axial extension can occur, and a peak in the J value in this region has been predicted theoretically for deep semi-elliptic cracks under tension **(11)**. In this test the assumption of a constant aspect ratio for the defect during ductile crack growth appears to be realistic, apart from near the outer surface.

Discussion

The main objective of this series of tests was to provide further validation of the R6 method. In this test, the defect was subject to a combination of primary stresses, and secondary residual welding stresses typical of an as-welded repair. Analysis has shown that at the deepest point of the defect, the residual stress will tend to close the crack, but would be unlikely to significantly affect the maximum pressure or the pressure for crack initiation. However, making conservative assumptions about the levels of residual stress, as is commonly done in practice if insufficient data on the actual residual stress profile are available, can grossly underestimate the load carrying capacity of the structure.

For the geometry under consideration, and a failure mode largely controlled by ligament collapse, the R6 method has safely underestimated the load carrying capacity of the structure by 9 percent, using best estimates of materials

properties and applied loads. Use of lower bound materials data would increase the conservatism of the analysis.

The sensitivity study has shown the importance of making realistic assumptions about the levels of residual stress, confirming the results of earlier work (3). The experiment has also demonstrated that residual stresses appear to have no effect once there is extensive plastic deformation in the remaining ligament, and this should be allowed for in assessments of structures failing at high values of L_r. If it can be shown that sufficient plastic deformation to remove any residual stresses can occur prior to failure, then it may be safe to neglect them. The possibility of elastic follow-up, i.e., the presence of longer range residual stresses which are not self-equilibrated across the section of interest, will always need to be investigated. Further work is necessary to devise general rules for the conditions when it is safe to neglect residual stresses. In many cases it may be preferable to obtain a better estimate of the level and form of residual stress present and including this in the defect assessment. The sensitivity study also showed the importance of accurate data other than stress data, if a realistic assessment is to be made. Uncertainties in materials properties, and knowledge of defect size and shape can be equally important.

The development of flaw shape in this test, both during fatigue pre-cracking and during pressurisation to failure can be explained in a qualitative way, and a simple analysis, modelling the defect as a semi-elliptic flaw, is able to give a good estimate of structural performance, without recourse to detailed finite element methods. In any defect assessment, there is no benefit in carrying out a detailed stress analysis if large uncertainties in material properties or defect size exist.

An important secondary objective which was fulfilled by this test was to show that an as-welded repair to a procedure suitable for use in the primary circuit of a PWR could be carried out, and shown to behave as predicted, in the presence of a defect. The high defect tolerance of the structure is well illustrated by a comparison of the actual failure pressure with that allowed by British Standard 5500 for a vessel of this geometry. The design pressure for an unflawed vessel is approximately 30 MPa, compared with an actual failure pressure of 83.4 MPa for this vessel containing a gross defect.

Conclusions

(1) The R6 assessment method has been shown to give a safe prediction of the performance of a pressure vessel containing a defect, using a realistic estimate of the residual stresses present.

(2) In practice, the residual welding stresses had a small effect on the pressure for crack initiation and on the maximum pressure sustained, and appear to be eliminated as plastic deformation develops in the remaining ligament.

(3) More information about the levels of residual stress for welds in common structural geometries would enable more accurate assessments to be made.

(4) The six layer repair technique for as-welded repairs in PWR primary pressure circuit components has been shown to give satisfactory and predictable performance.

Acknowledgements

This work was carried out at the Central Electricity Research Laboratories and permission to publish was given by the Central Electricity Generating Board. The author is grateful to Babcock Power Research Centre for carrying out the pressure test, and to Mr D. J. Southall for assistance with post test analysis.

References

(1) MILNE, I., AINSWORTH, R. A., DOWLING, A. R., and STEWART, A. T. (1986) Assessment of the integrity of structures containing defects, CEGB Report R/H/R6, Revision 3.

(2) MILNE, I. and KNEE, N. (1988) Report on EGF Task Group I exercise in predicting ductile instability. Phase II: Experimental cracked pressure vessel, *Fatigue Fracture Engng Mater. Structures*, **9**, 231–257.

(3) KNEE, N. and MILNE, I. (1985) Stable crack extension from semi-elliptic defects in the presence of residual welding stresses, Proc. Conf. on Effects of Fabrication Related Stresses, Paper **41**, Cambridge.

(4) KNEE, N. (1986) Report on phase IV of the European Fracture Group round robin exercise on the prediction of ductile instability, *Fracture Mechanics of Welds*, EGF 2 (Edited by J. H. Blauel and K.-H. Schwalbe), Mechanical Engineering Publications, London.

(5) BABCOCK and WILCOX COMPANY (1984) Repair welding of heavy-section steel components in LWRs, *EPRI Report NP-3614*, Volume **1**, Summary.

(6) NIX, K. J., KNEE, N., LINDLEY, T. C., and CHELL, G. G. (1988) An investigation of fatigue crack growth in a ductile material at high growth rates, *Fatigue Fracture Engng Mater. Structures*, **11**, 205–220.

(7) LEGGATT, R. H. (1986) Residual stress measurements at repair welds in pressure vessel steels in the as-welded condition, Welding Institute Research Report 315/1986.

(8) RAJU, J. S. and NEWMAN, J. C., Trans. ASME (1982) *J. Pressure Vessel Technol.*, **104**, 293–298.

(9) KIEFNER, J. F., MAXEY, W. A., EIBER, R. T., and DUFFY, A. R. (1973) Progress in flaw growth and fracture toughness testing, *ASTM STP 536*, ASTM, Philadelphia, pp. 461–481.

(10) BRYAN, R. H., BASS, B. R., BRYSON, J. W., and MERKLE, J. G. (1984) Experimental investigation of tearing behaviour of a flaw in a thick pressure vessel, *Light Water Reactor Structural Integrity*, (Edited by K. E. Stahlkopf and L. E. Steele) Elsevier, New York, pp. 175–209.

(11) YAGAWA, G., UEDA, H., and TAKAHASHI, Y. (1986) Numerical and experimental study on ductile fracture of plate with surface crack, ASME Conf. on Pressure Vessels and Piping, ASME, New York, Vol. 103, pp. 43–48.